Chemical Engineering Journal 158 (2010) 11–18

Contents lists available at ScienceDirect

Chemical Engineering Journal

journal homepage: www.elsevier.com/locate/cej

Studies of the flow in and around gas dedusters and demisters using neutrally buoyant tracer

Weiming Peng, Dorthe Christensen, Siri Jacobsson, Eli Kvinnesland, Alex C. Hoffmann*

Department of Physics and Technology, University of Bergen, Norway

ARTICLE INFO

Article history:
Received 7 April 2008
Accepted 3 July 2008

Keywords:
Gas-cleaning equipment
Flow
Vortex
Neutrally buoyant tracer

ABSTRACT

Tracer studies of the flow in gas dedusting or demisting equipment is a problem area, since such equipment is designed to cause the paths of solid or liquid particles to deviate from the gas streamlines, conflicting with the purpose of tracer particles. This paper summarizes a number of studies of the flow in centrifugal gas cleaning equipment using neutrally buoyant tracer particles, which are helium-filled soap bubbles about 1 mm in size. The studies show vortex precession in the body of reverse-flow cyclones, vortex breakdown in the vortex finder of reverse-flow cyclones and after the outlet of once-through cyclones. They also show other features of the flow in gas cleaning equipment not visualized before. Most of the results shown a qualitative, illustrating the potential of this visualization technique.

1. Introduction

Tracer visualization and laser-Doppler anemometry (LDA) studies of the flow in gas dedusting or demisting equipment is a problem area. If the equipment is working in accordance with its purpose, solid or liquid tracer particles will tend to deviate from the gas streamlines, and may even be collected in the equipment. For instance, it is normally not possible to study the core of the vortex in centrifugal gas cleaning equipment by visualization, since tracer particles—even sub-micron ones—are centrifuged radially outward to the outer part of the vortex, or even to the wall of the separator. For the same reason, it is not reliable to determine the radial gas velocity in such equipment using LDA.

LDA studies of the axial and circumferential gas velocity components in cyclones and swirl tubes are reported in the recent papers of Refs. [9,8]. In the latter reference, detailed maps of the axial and tangential velocity components and the RMS turbulent velocity around the dust exit region are shown.

While LDA will give the instantaneous and also the time–mean velocity at a point, flow visualization, as a complement to LDA, offers the advantage of direct observation of the flow pattern in the device, and the recording of the flow pattern by photographic techniques. Flow visualization can reveal features of the flow that LDA cannot, for instance the periodic movement due to precession of a vortex core will not easily be picked up by LDA, but will be evident with flow visualization.

Due to the above-mentioned difficulties with tracer particles, only very few flow visualization studies of dedusting or demisting equipment have been published. Wakelin [13] performed a pioneering study, where he used, among other tracers, neutrally buoyant tracer bubbles to study the flow pattern in centrifugal separation equipment. He studied many aspects of the flow pattern, such as the near-wall secondary flows and the radial inward flow, and the end-of-the-vortex phenomenon.

This article summarizes results obtained with flow visualization using neutral-density helium-bubble tracer. Some of the results shown have been discussed in detail in other publications [12,6], which focus on specific sub-topics.

2. Experimental technique

The helium-bubble generator used is from Sage Action Inc. It produces helium-filled, neutrally buoyant bubbles. These bubbles are, in general, stable at gas velocities up to about 70 m/s. The tracer bubbles are illuminated with a 300-W tungsten–halogen lamp. A small cyclone in the bubble generator allows only neutrally buoyant tracer through; bubbles that are too dense or too light impact on the outer wall or on the vortex finder (see Fig. 1 below) of the device, respectively.

The flow pattern was recorded by photographic techniques. For visualization of the flow, controlled exposure times were used to record tracer paths as streaks on the image. Various techniques for obtaining velocity information were tried out, among other things measuring the streak length left by tracer particles on images with

* Corresponding author at: Department of Physics and Technology, University of Bergen, Allegaten 55, Bergen 5007, Norway. Tel.: +47 5558 2876; fax: +47 5558 9440.
E-mail address: Alex.Hoffmann@ift.uib.no (A.C. Hoffmann).

1385-8947/$ – see front matter © 2008 Elsevier B.V. All rights reserved.
doi:10.1016/j.cej.2008.07.014

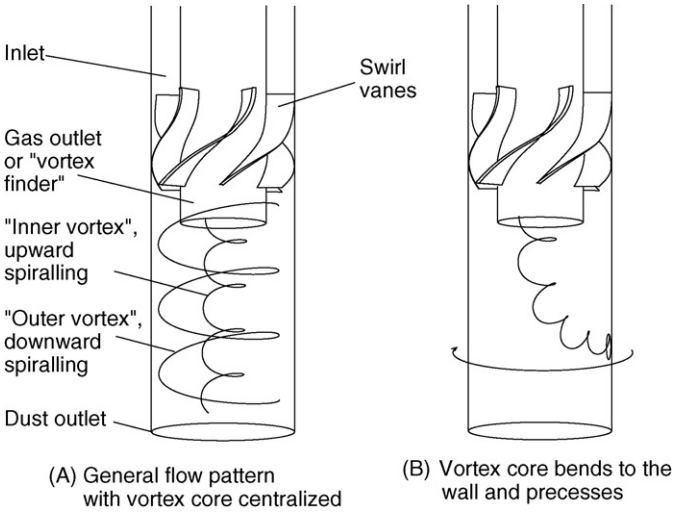

Fig. 1. (A) Schematic showing the general flow configuration in a reverse-flow swirl tube. (B) Illustration of the flow when the vortex ends in the separation space. The vortex core bends to—and precesses around—the wall.

a known exposure time. The most successful in terms of analysis, at least within the confines of this project, turned out to be filming the flow with a high-speed video camera and identifying the same tracer particles on successive frames, the distance travelled between the frames giving the velocity.

3. Neutrally buoyant tracer in a strongly swirling gas flow

Since the over-all density of the helium-bubbles is the same as air as they emanate from the bubble generator, their terminal velocity relative to the air is zero: $(\mathbf{u}-\mathbf{v})$, with $\mathbf{u}$ and $\mathbf{v}$ the bubble and air velocities, respectively. The only difference between the bubbles and air pockets of a similar size is that the bubbles will not shear. The bubbles should therefore follow the motion of the air faithfully. They should even follow the motion of the turbulent eddies, at least for eddies larger than size of the bubble itself. The Kolmogorov length scale for the size of the smallest eddies can be estimated from the empirical equation:

$$l_K = 4D\,Re^{-0.78} \tag{1}$$

where Re is the Reynolds number for the flow: $\rho_g v D/\mu_g$, v is some characteristic gas velocity, D a characteristic dimension, e.g. the diameter of the vessel, and μ_g and ρ_g the gas viscosity and density, respectively. Using order-of-magnitude estimates of 10 m/s and 0.1 m for v and D, and 1.2 kg/m^3 and 1.8 $\times 10^{-5}$ Pa s for ρ_g and μ_g, gives about 70 μm for the Kolmogorov length scale. The size of the tracer bubbles was typically around 1 mm. However, 1 mm is well within the dissipative range of the turbulence, and eddies smaller than this do not have a strong effect on the flow.

In the gas motion in a deduster or demister, strong gradients in the air velocity exist, giving rise to rotation of the bubbles. We can consider if lift forces might act on the bubbles, causing them to move, for instance, inward or outward in a vortex. Crowe et al.[2] mention two types of lift force: the Magnus force, which arises due to rotation of the particle, and the Saffman force, which arises due to velocity gradients in the air itself.

At low particle Reynolds number (which we always have with he-bubbles), the Magnus force is given by [2]:

$$F_{mag} = \frac{\pi}{8} D^3 \rho \left[\left(\frac{1}{2} \nabla \times \mathbf{u} - \boldsymbol{\omega}_d \right) \times (\mathbf{u}-\mathbf{v}) \right]. \tag{2}$$

The Saffman force, again at low particle Reynolds number, is:

$$F_{saff} = 1.61 D^2 \sqrt{\frac{\mu \rho_p}{|\nabla \times \mathbf{u}|}} [(\mathbf{u}-\mathbf{v}) \times |\nabla \times \mathbf{u}|]. \tag{3}$$

The existence of both lift forces depend on the existence of a relative velocity between the particle and gas $(\mathbf{u}-\mathbf{v})$, and are therefore absent in the case of the he-bubbles, and we can thus expect the he-bubbles to follow the gas flow faithfully, even to the extent of following the turbulent eddies except for the very smallest eddies.

4. Results and discussion: flow visualization

We discuss the results of visualizations of various flow configurations and features separately in this section.

4.1. The vortex core in centrifugal gas cleaning equipment

One significant advantage of using approximately neutrally buoyant he-bubbles as tracer is that some bubbles, slightly less than neutrally buoyant, will collect at the core of the vortex, and make this visible. Whether this happens or not, and to which extent, can be controlled by tweaking the bubble generator to adjust the buoyancy of the bubbles precisely. Fig. 1 A shows the general flow pattern in a cylindrical centrifugal separator with swirl vanes, often referred to as a "swirl tube".

One flow feature, which is critical for the design and operation of reverse-flow centrifugal separators is the so-called end of the vortex. This is a position low in, or under, the separation space, where the vortex motion suddenly stops or becomes much reduced, often visible by the formation of a ring in the dust striation pattern during operation, or in the dust deposition pattern after operation. If this end of the vortex occurs in the separation space, this can lead to problems such as inferior separation, wear, clogging or "cross-talk" between cyclones working in parallel over a common dust hopper [10]. The nature of this phenomenon was recently established [11], and the principle is illustrated in Fig. 1 B.

Fig. 2 shows the core of the vortex in a swirl tube (internal diameter, $D = 110$ mm) in which the core is centralized, i.e. it coincides, at least roughly, with the central axis of the tube. The vortex ends on the bottom of the dust collection chamber, even though the diameter of this is significantly larger than that of the tube itself, something that will normally destabilize the vortex (see below).

Fig. 3 shows a case where the vortex core deviates from the axis of the swirl tube, bends to the wall, and precesses around the wall at the point of the "end of the vortex". Due to the fast precession, the core appears as a conical shape to the naked eye, and on images with a reasonably long exposure time. The plates to the right show the vortex core at two different levels visualized from above. The irregular particle paths in these two plates are evidence of the radial turbulence.

The vortex end is thus not associated with vortex breakdown internally in the fluid. However, the he-bubble tracer technique does allow observation of vortex breakdown. We will describe two flow configurations where we believe we are seeing this.

The first flow configuration is the flow in a conical vortex finder. Fig. 4 shows how the pathlines of the helium bubbles widen in the (conical) vortex finder of a swirl tube, indicating the existence of a type "0" [4] vortex breakdown in the vortex finder.

That such a breakdown should exist under some conditions in the vortex finder of a reverse-flow centrifugal separator is supported by the recent numerical study of Ref.[3], wherein large eddy CFD simulations show such a breakdown to occur in a vortex-finder-like feature of a vortex tube.

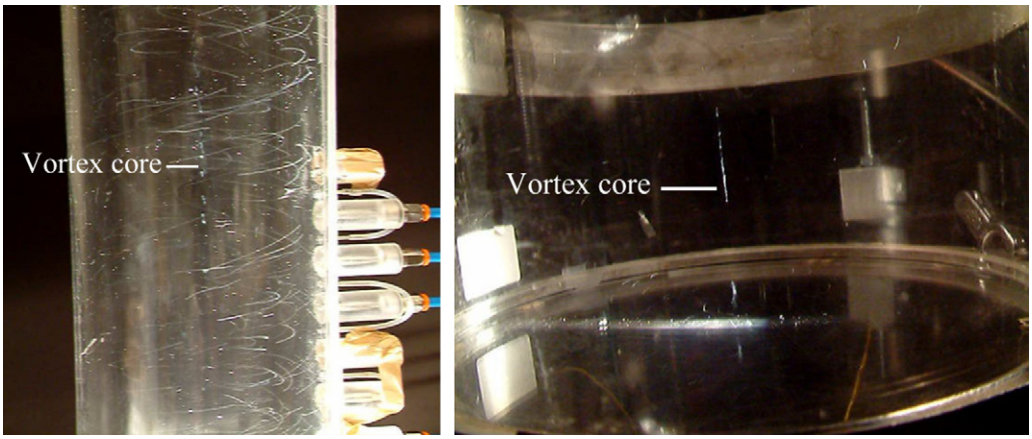

Fig. 2. Left: the vortex core in the separation space of a swirl tube separator; the core is visible due to some light bubbles concentrating in the core, other bubbles can be seen in the outer part of the vortex. Right: the core manages to negotiate a dust collection vessel under the swirl tube, even though the collection vessel is wider than the tube, and ends on the bottom of the collection vessel.

A similar feature was observed downstream of a straight-through swirl tube. In such a tube, the gas flow exits at the same end of the separator as the separated particles or liquid. It is important to know what happens to the vortex downstream of such tubes, for instance arranged in parallel in a natural gas scrubber. Fig. 5 shows this phenomenon downstream of the straight-through swirl tube ($D = 80$ mm) with upward flow [5]. In most of the pictures taken of this phenomenon it was not possible to determine whether the vortex core as a whole was rotating, or the individual streamlines were diverging around a type "0" breakdown. It can be seen, however, in these images taken with a very low exposure time that the individual streamlines diverge, this is especially clear in the image to the right. In this and some of the subsequent images it is clear that each bubble reflects the illumination in two points, giving rise to twin path-lines on the images. The spatial separation of these twin paths depends on the size of the bubbles and on the angle of the illumination relative to that of the camera.

Fig. 6 also shows the flowpattern downstream of the tube in Fig. 5, but photographed from above using horizontal light sheets for illumination. In the left photo the light sheet is just above the exit from the swirl tube showing again the rotation in the exiting, down-breaking vortex, while the right one it is higher in the large, square chamber downstream of the tube showing that vortex motion is largely absent there.

4.2. Inner vortex boundary

The vortex in a reverse-flow centrifugal separator is often said to consist of an "outer vortex" with downward spiralling flow, of the diameter of the separator, D, and an "inner vortex" with upward

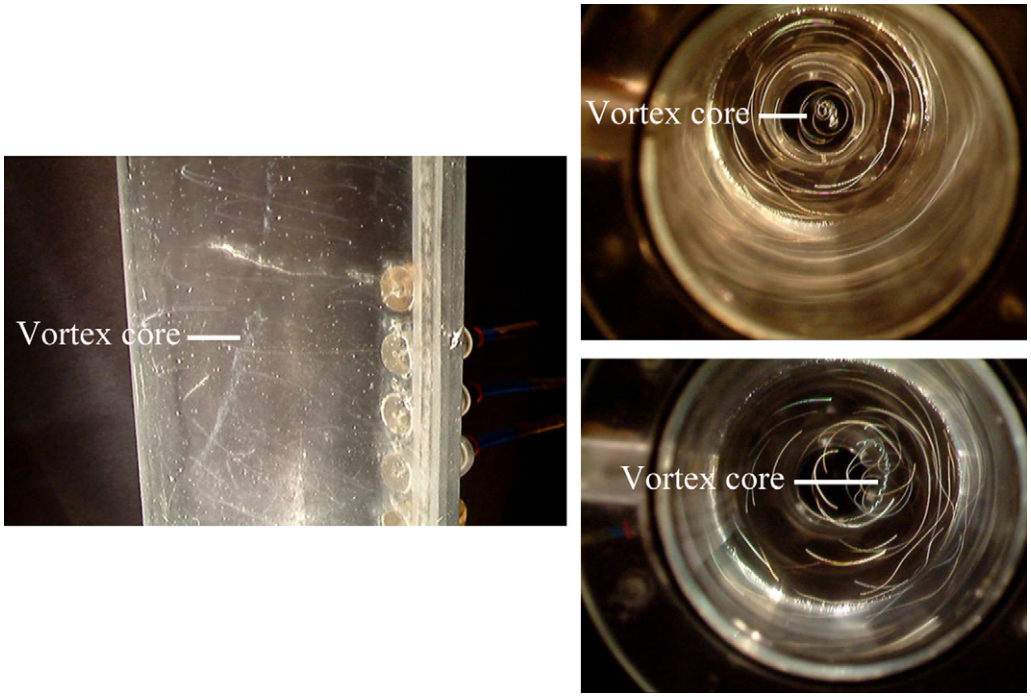

Fig. 3. Left: the conical shape formed by the precessing vortex core. Top right: a photo taken from the bottom of the swirl tube illuminated with a horizontal light sheet rather high in the tube, where the core is still centralized. Bottom right: the light sheet is placed lower in the tube, closer to the position of the "vortex end", where the core is no longer centralized.

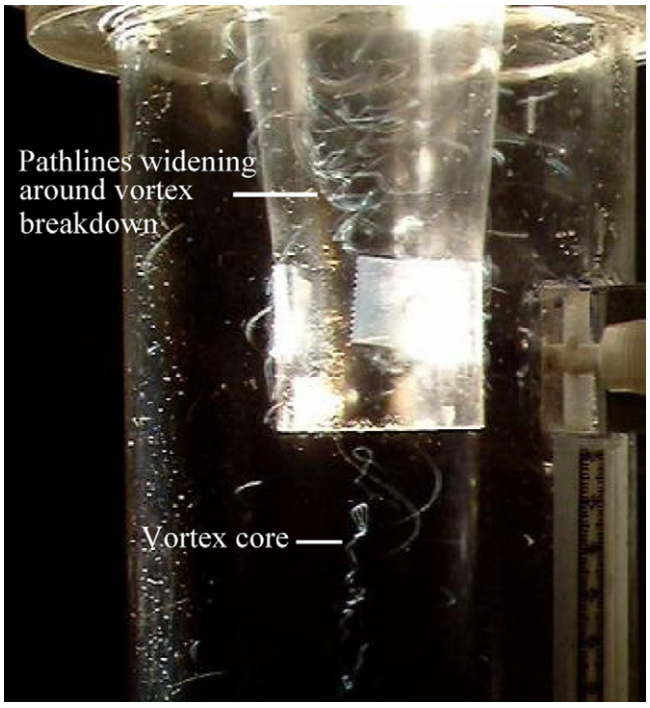

Fig. 4. The widening pathlines of the helium tracer bubbles indicate a type "0" vortex breakdown in the conical vortex finder of a swirl tube.

spiralling flow with a diameter approximately equal to that of the vortex finder, D_x. If photos are taken of the vortex at some oblique angle to the separator axis, the pathlines of tracer should be distinguishable between the two.

At present, we only have photos taken at right angles to the separator axis. Even in such photos, however, the inner and outer vortices may be distinguishable. If we use the well-known "n-law" for the swirl velocity, v_θ, in the vortex, and denote the inner and outer vortex by subscript iv and ov, respectively, we can estimate that

$$v_\theta = \frac{C}{r^n} \approx \frac{C}{r^{0.8}} \Rightarrow \frac{v_{\theta,\mathrm{iv}}}{v_{\theta,\mathrm{ov}}} = \left(\frac{D}{D_x}\right)^{0.8}. \quad (4)$$

For the vertical velocities, v_z in the two parts of the vortex, we can, at least for the part of the vortex just under the lip of the vortex finder, estimate

$$\frac{v_{z,\mathrm{iv}}}{v_{z,\mathrm{ov}}} = \frac{A_{\mathrm{ov}}}{A_{\mathrm{iv}}} = \frac{(D^2 - D_x^2)}{D_x^2}. \quad (5)$$

Fig. 7 shows an image of the vortex just under the lip of the vortex finder in a reverse-flow swirl tube with $D = 110$ mm and $D_x = 59$ mm, giving $v_{\theta,\mathrm{iv}}/v_{\theta,\mathrm{ov}} \approx 1.6$ and $v_{z,\mathrm{iv}}/v_{z,\mathrm{ov}} \approx 2.5$. Thus, the vertical velocity is higher relative to the swirl velocity in the inner vortex than in the outer. We think that we see this in the photo shown in Fig. 7.

4.3. The flow around two natural gas scrubber inlet types

Neutral buoyancy tracer allows the study of many other flow configurations in and around gas–solid or gas–liquid separators. The vane-type inlet to a gas scrubber is designed to dissipate the momentum of the incoming liquid-laden gas, distribute the gas through its sides evenly over the scrubber cross-section, and separate some of the droplets. To effect the capture, the liquid-laden gas is turned sharply by the vanes, causing the droplets to impact on the vanes. This feature, however, makes it very difficult to study the flow emanating from the inlet by conventional tracer techniques. Fig. 8 shows the flow emanating from the sides of a vaned inlet to a natural gas scrubber using he-bubble tracer [7].

Fig. 9 shows a simulation using FLUENT of the flow through the vaned inlet, note the similarity with the right-hand picture of Fig. 8.

Another, patented, type of scrubber inlet is shown in Fig. 10[1]. This inlet configuration is designed to bring the incoming gas into a downwardly swirling motion in the outer, lower channel. Some gas escapes into the inner part through the slit, and a swirling motion (anticlockwise when seen from above) results in the lower part and under the inlet, separating droplets to the wall. All the gas eventually leaves the inlet upwards, and the axial flow is upward in the inner part of the device. In the upper part some gas will escape to the out part through the slits, and this will be forced to rotate clockwise.

The left photo in Fig. 11 shows the flow in the lower part—but within the inlet, confirming that there is a strong swirling motion in the gas. This was taken using a light sheet inclined to match the slit in the lower part. The right photo shows the flow just above the inlet, confirming that the strong swirling motion is dissipated by the

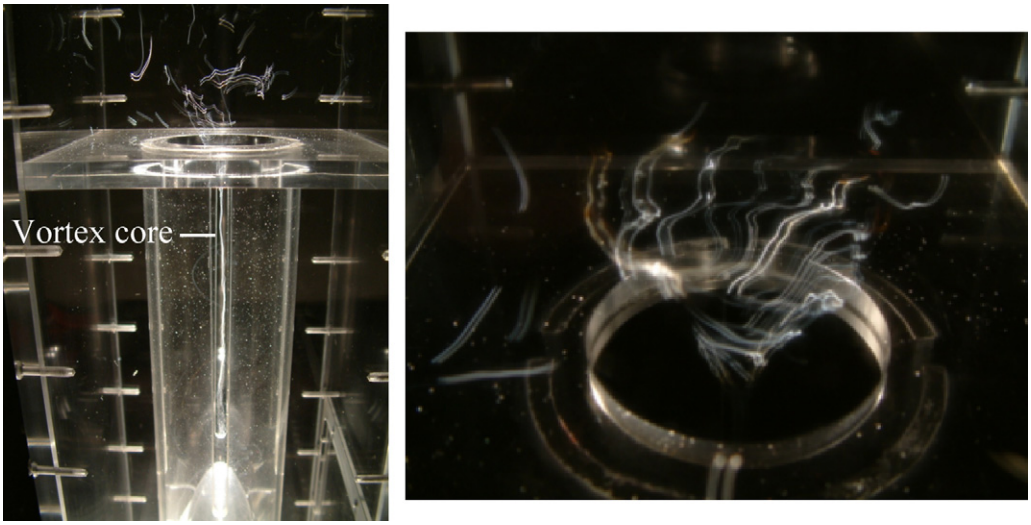

Fig. 5. Vortex breakdown downstream of a straight-through swirl tube separator.

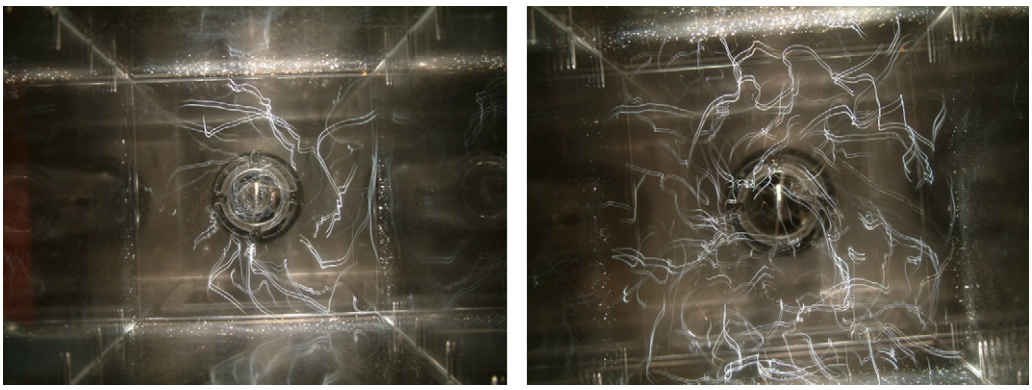

Fig. 6. Vortex breakdown downstream of a straight-through swirl tube separator photographed from above. Top: flow just above the tube, bottom: flow further downstream.

Fig. 7. Boundary between the inner and the outer vortex.

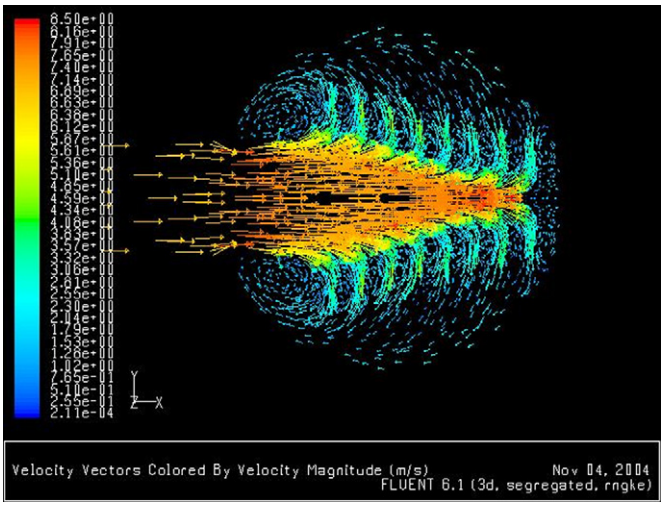

Fig. 9. Simulation of the flow through the vaned inlet using FLUENT.

Fig. 8. Flow around the vaned inlet to a gas scrubber. The internal diameter of the cylinder housing the inlet is 150 mm. To the right, the whole vaned inlet assembly is seen, with the flow from the vanes at the side, continuing in a rather turbulent by evenly distributed manner above the vane. To the left a detail of the flow emanating from the vanes.

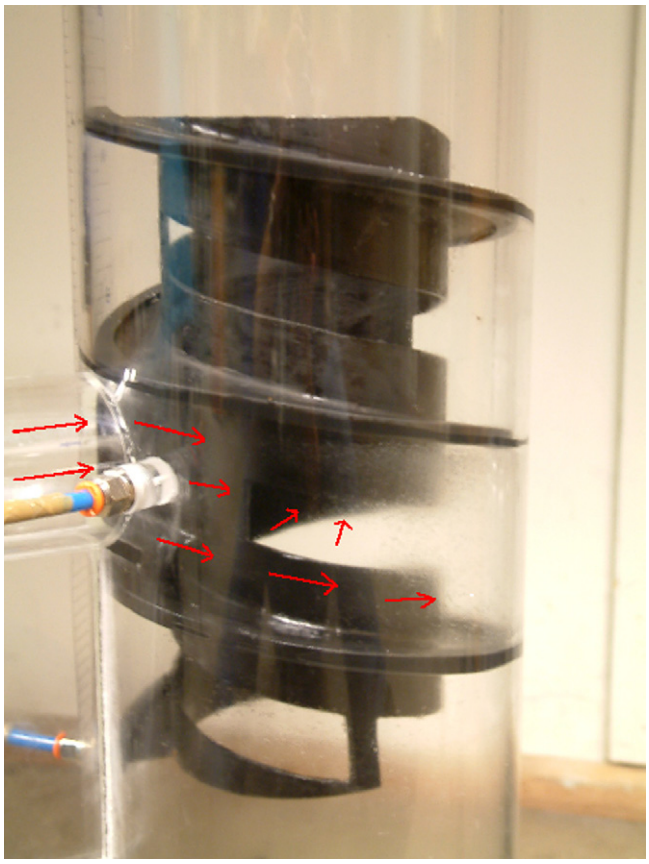

Fig. 10. Inlet device causing the droplet-laden gas to spin.

counter-rotation of the gas flow emanating from the outer channel. Video analysis confirms this counter-rotation. It should be noted that further from the inlet, rotation is to some extent reestablished, perhaps due to the counterclockwise momentum being the greater.

Fig. 12 shows a detail of the flow in this inlet, where the flow through the slit from the outer to the inner part of the inlet, just after the gas enters the device, was captured.

5. Some approaches to quantification of the flow field

A number of techniques for quantifying the flow fields (determining the velocity fields) were attempted, most of them with a measure of success:

Fig. 12. Detail of the flow in the inlet shown in Fig. 10.

- Measuring the length of streak lines on photographs with known exposure time. Known exposure time was achieved by:
  - Known camera aperture time with continuous illumination.
  - Known illumination time with long camera aperture time. For this the illumination was flashed several times during the camera aperture time, and the flashes took the form of:
    (i) Even streaks (– – –).
    (ii) Coded streaks to glean also the direction of velocity (· – · –).
- Measuring the distance between the images of same bubble on successive exposures in a high-speed film.

In all cases the light was white, and was in the form of a sheet, such that velocities in a reasonably well-defined plane were obtained. Fig. 13 shows the screen rotated in front of the light source to generate coded streaks, and a corresponding image to the right. Notice how some of the bubbles are significantly accelerated or decelerated during their flight.

We ended up using the last of the options listed above in this work, mainly because of time constraints limiting the in-house development of software. Thus we used high-speed-video imaging combined with analysis of subsequent frames. The analysis software acquired for this was DiaTrack 2.3 from SemaSopht.

The analysis procedure is roughly as follows. The first frame of a sequence is loaded, and pre-processed, for optimally contrasting the particles that are to be tracked. Objects that do not fulfil certain

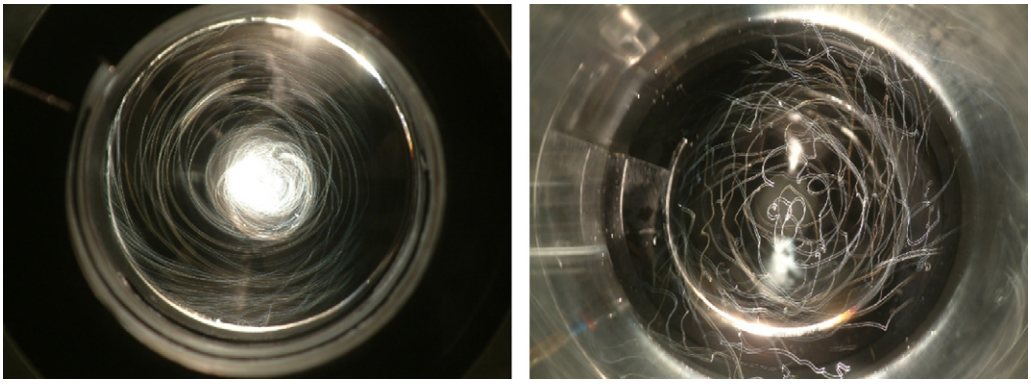

Fig. 11. Flow pattern in horizontal planes around the inlet in Fig. 10. Left: in the lower part of the inlet. Right: just above the inlet.

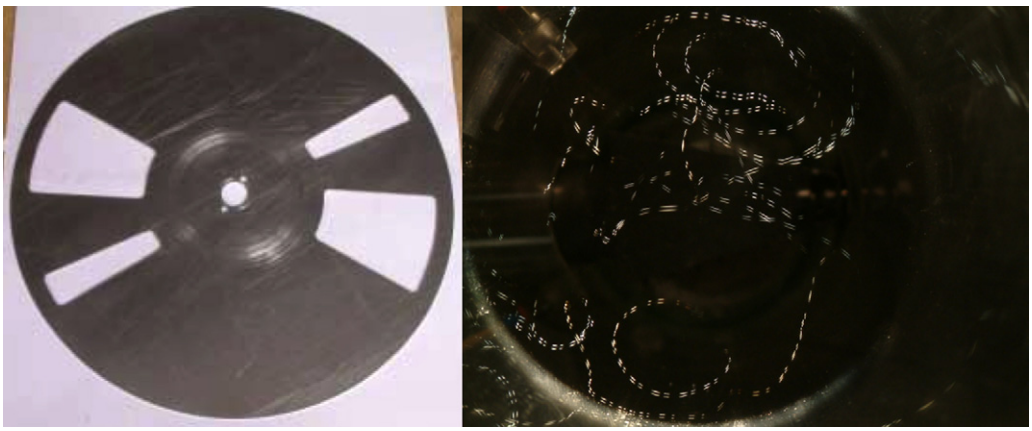

Fig. 13. Left: the screen rotated in front of the continuous white-light source to generate coded streaks from the tracer on photographic images. The light was caused to form a sheet by a second, stationary, screen. Right: an example of the resulting images.

criteria set are removed. When the user is satisfied the program can automatically repeat the same operations for all successive images, each of the particles identified can be recognized in all the frames and matched between the frames to produce the trajectories. This, however, demands some operator judgement and skill, and work aimed at automatizing the particle identification on each frame and the particle recognition between frames is urgently needed for this method to become more generally useful. A panel of postprocessing tools allows a range of quantitative analyses, although fine-turning of the averaging method was not possible in the version we used.

The left-hand plates in Figs. 14 and 15 show the type of raw data obtained from the analyses. Several arrowheads can be seen along

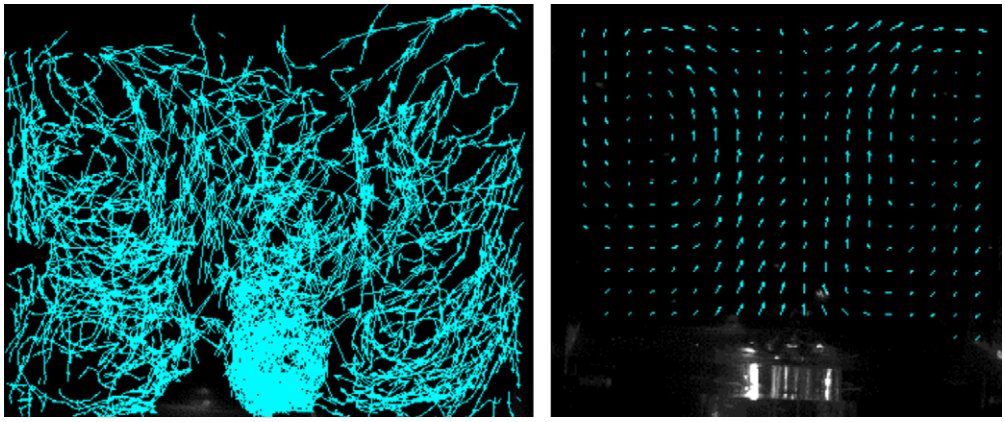

Fig. 14. Flow pattern downstream of the tube in a vertical slice through the axis of a straight-through swirl tube. Left: the raw data from the he-bubble tracking. Right: averaged flow pattern [5].

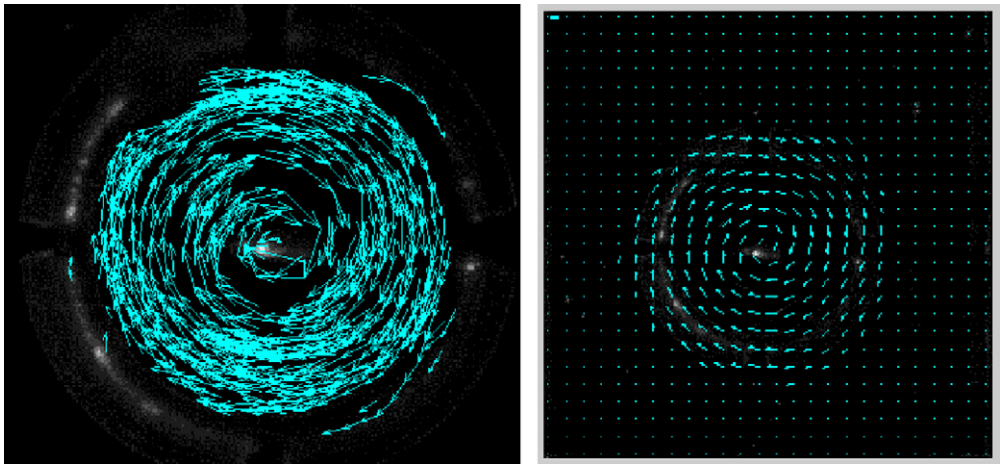

Fig. 15. Flow in a horizontal slice in the separation space of a straight-through swirl tube. Left: raw data from the he-bubble tracking. Right: averaged flow pattern [5].

each particle path, showing that several subsequent frames were included in the analysis.

The right-hand plates in these two figures show the averaged velocity fields calculated from the images, Fig. 14 in a vertical slice above the straight-through swirl tube, and Fig. 15 in a horizontal slice in the swirl tube itself.

6. Conclusions

- Flow visualization with neutral-density tracer makes it possible to visualize many features of the flow pattern in gas–solid or gas–liquid separators, which otherwise could not be observed.
- The "end of the vortex" phenomenon low in centrifugal separators does not involve vortex breakdown internally in the fluid.
- Vortex breakdown of the type "0" ("bubble-type") was observed in the (conical) vortex finder of a separator, and downstream of a straight-through swirl tube separator.
- Quantification of the flow field was possible by identifying tracer bubbles between frames, but this method still requires research aimed a automatization.

Acknowledgements

Financial support from Shell Global Solutions and from the Research Council of Norway through the HiPGaS programme, and the industrial sponsors Statoil AS, ConocoPhillips, Norsk Hydro AS, Vetco, FMC Kongsberg Subsea and Aker Solutions is highly appreciated.

References

[1] D. Christensen, 2005. Single-phase characterization of the new open spinlet arrangement, Master's Thesis, University of Bergen, Dept. of Physics and Technology.
[2] C. Crowe, M. Sommerfeld, Y. Tsuji, Multiphase Flow With Droplets and Particles, CRC Press, Boca Raton, 1998.
[3] J.J. Derksen, Simulations of confined turbulent vortex flow, Comp. Fluids 34 (2005) 301–318.
[4] J.H. Faler, S. Leibovich, Disrupted states of vortex flow and vortex breakdown, Phys. of Fluids 20 (1977) 1385–1400.
[5] S. Jacobsson, 2005. Single-phase characterization of the verlaan cyclone, Master's Thesis, University of Bergen, Dept. of Physics and Technology.
[6] S. Jacobsson, T. Austrheim, A.C. Hoffmann, Experimental and cfd investigation of the flow in and around once-through swirl tubes, Ind. Eng. Chem. Res. 45 (2006) 6525–6530.
[7] E. Kvinnesland, 2005. Single-phase characterization of the inlet arrangement schoepentoeter, Master's Thesis, University of Bergen, Dept. of Physics and Technology.
[8] S. Obermair, J. Woisetschläger, G. Staudinger, Investigation of the flow pattern in different dust outlet geometries of a gas cyclone by laser doppler anemometry, Powder Technol. 138 (2003) 239–251.
[9] W. Peng, A.C. Hoffmann, P. Boot, A. Udding, H.W.A. Dries, A. Ekker, J. Kater, Flowpattern in reverse-flow centrifugal separators, Powder Technol. 127 (2002) 212–222.
[10] W. Peng, A.C. Hoffmann, H.W.A. Dries, M.A. Regelink, K.-K. Foo, Reverse-flow, centrifugal separators operating in parallel, performance and flow pattern, AIChE J. 53 (2007) 589–597.
[11] W. Peng, A.C. Hoffmann, H.W.A. Dries, M.A. Regelink, L.E. Stein, Experimental study of the vortex end in centrifugal separators: The nature of the vortex end, Chem. Eng. Sci. 60 (2005) 6919–6928.
[12] W. Peng, A.C. Hoffmann, H.W.A. Dries, M. Regelink, K.-K. Foo, Neutrally boyant tracer in gas celaning equipment. a case study, Meas. Sci. Technol. 16 (2005) 2405–2414.
[13] R. Wakelin, 1992. Vortex breakdown in dust-collecting return-flow cyclones, PhD Thesis, University of Canterbury.